

The Binding Mode of Epothilone A on α,β -Tubulin by Electron Crystallography

James H. Nettles,¹ Huilin Li,² Ben Cornett,³ Joseph M. Krahn,⁴
James P. Snyder,^{3*} Kenneth H. Downing^{5*}

The structure of epothilone A, bound to α,β -tubulin in zinc-stabilized sheets, was determined by a combination of electron crystallography at 2.89 angstrom resolution and nuclear magnetic resonance-based conformational analysis. The complex explains both the broad-based epothilone structure-activity relationship and the known mutational resistance profile. Comparison with Taxol shows that the longstanding expectation of a common pharmacophore is not met, because each ligand exploits the tubulin-binding pocket in a unique and independent manner.

The extraordinary clinical success achieved by Taxol (1) and related taxanes in treating a wide variety of cancers has been accompanied by delivery problems (1), resistance arising from various cellular factors, including increased P-glycoprotein expression (2), and numerous side effects (3). A search for alternative drug therapies that also operate by microtubule stabilization has led to a focus on a family of 16-membered ring macrocyclic lactones represented by epothilone A (EpoA, 2) (Scheme 1). Discovered by Höfle and co-workers from the myxobacterium *Sorangium cellulosum* (4), epothilones are more water soluble than Taxol, appear to largely escape drug resistance encountered by taxanes, and cause tumor cell death by stabilizing microtubules and inducing apoptosis (5).

Since the discovery of the epothilones in 1993, an impressive structure-activity relationship (SAR) profile has emerged from the efforts of numerous synthetic teams (6). Epothilones, Taxol, and other microtubule stabilizers, including the endogenous neuronal tau protein (7), compete for the same binding pocket on β -tubulin. This has prompted attempts to describe a common pharmacophore for the structurally diverse taxanes and epothilones (8–11). This exercise, pursued primarily to facilitate the rational design of chemotherapeutic agents, is based on the assumption that superimposable polar and hydrophobic groups on the individ-

ual ligands interact with complementary subsites on the protein target.

Combining nuclear magnetic resonance (NMR) spectroscopy, electron crystallography (EC), and molecular modeling (12), we derived a structural model of the binding mode and conformation of EpoA in complex with the β -tubulin subunit in zinc-stabilized tubulin sheets (Fig. 1). A similar approach has led to the identification of T-Taxol: Taxol bound to β -tubulin in a conformer with approximately equal distances between the C-2 phenyl and the two C-3' aromatic substituents (13). The complex accommodates the extensive epothilone SAR data developed for microtubules composed of wild-type tubulin (TB) and the more limited resistance data from mutant tubulins. Importantly, the structure demonstrates that, whereas EpoA and Taxol overlap in their occupation of a rather expansive common binding site on tubulin, the expectation of a common pharmacophore is unmet, because each ligand exploits the

binding pocket in a unique and qualitatively independent manner (Fig. 2).

A variety of epothilone conformations and binding modes on tubulin have been proposed by pharmacophore mapping (10, 11), solution NMR (14, 15), and the superposition of epothilones on Taxol or Taxotere in the EC tubulin complex (8, 9). All proposals for the binding mode have assumed that the macrocyclic epothilone ring occupies common space with the baccatin core of Taxol, whereas the thiazole side chain superposes one of its three phenyl rings. Thus, He (8) and Giannakakou (9) placed the C-2 benzoyl phenyl, Giannakakou and Wang (9, 10) the C-3' phenyl, and Ojima (11) located the C-3' benzamido phenyl as coincident with the thiazole ring. Overlap of the two drugs' binding modes determined by EC illustrates that the thiazole of EpoA benzoyl phenyl resides in a region of the tubulin pocket unoccupied by Taxol (Fig. 2). Of the five oxygen-containing polar groups decorating the epothilone macrocycle, only C7-OH falls near the similar C7-OH moiety in paclitaxel (Fig. 2), making this center the only notable common non-bonded contact for the two molecules. With one exception (10), all previous proposals have directed the C12–C13 epoxide ring outward from the periphery of the molecule. This is in marked contrast to the C10–C15 fragment that is folded beneath the macrocycle and above the hydrophobic pocket in the present model (Figs. 1 and 3). As previously speculated (10), the lack of protein-ligand interaction with the epoxide ring is consistent with the activity of olefin analogs EpoC and EpoD lacking the oxygen. Complementing the epoxide fold is a near-parallel orientation of the C–O bonds at C3, C5, and C7, an alignment ideal for the ligand-tubulin interaction. This arrangement leads to a very different set of backbone torsion angles from

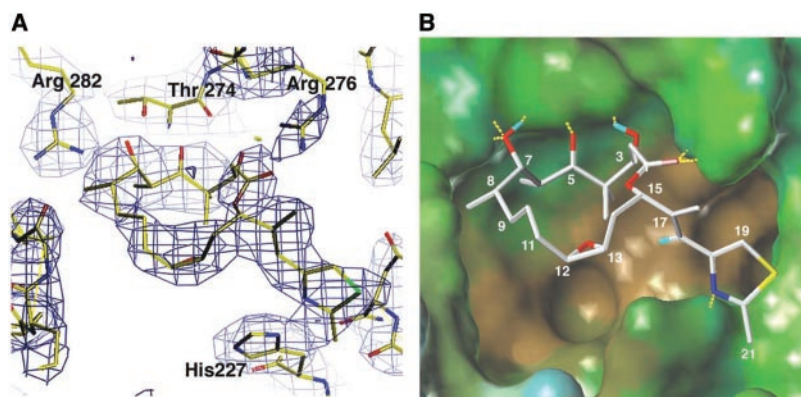


Fig. 1. (A) The density map (purple wireframe) resulting from Fourier synthesis of the EC diffractions ($2F_{\text{obs}} - F_{\text{calc}}$) and associated model (stick figure is colored by atom type: yellow, C; red, O; blue, N; and green, S) derived from electron crystallographic analysis of epothilone A (1) bound to zinc-stabilized two-dimensional crystals of tubulin. **(B)** Hydrophobic (brown) to hydrophilic (blue) properties are mapped to the solvent-accessible β -tubulin surface at the ligand-binding site. Epothilone A (white, C; red, O; blue, N; and yellow, S) is shown with hydrogen bonds (yellow dashes) to associated centers on the β -tubulin protein. Select hydrogens (cyan) are also modeled.

¹Molecular and Systems Pharmacology, Emory University, Atlanta, GA 30322, USA. ²Department of Biology, Brookhaven National Laboratory, Upton, NY 11973, USA. ³Department of Chemistry, Emory University, Atlanta, GA 30322, USA. ⁴Laboratory of Structural Biology, National Institute of Environmental Health Sciences, Research Triangle Park, NC 27709, USA. ⁵Life Sciences Division, Lawrence Berkeley National Laboratory, Berkeley, CA 94720, USA.

*To whom correspondence should be addressed. E-mail: snyder@euch4e.chem.emory.edu (J.P.S.); khdowning@lbl.gov (K.H.D.)

C1 to C9 for epothilone A in comparison with either its single crystal x-ray structure or the transfer nuclear Overhauser effect NMR structure of EpoA, completed with an unpolymerized soluble form of the protein (14).

Six residues lining or adjacent to the ligand-binding pocket in β -tubulin undergo mutation under pressure from exposure of various cell lines to epothilones (Ala²³¹, Thr²⁷⁴, Arg²⁸², and Gln²⁹²) (9, 16, 17) or taxanes (Phe²⁷⁰ and Ala³⁶⁴) (18). Superposition of the two ligands along with the corresponding β -tubulin side chains provides a graphical portrait of the origins of the observed differential acquired resistance (fig. S7). For example, Taxol's C3'-phenyl and C4-OAc are in van der Waals contact with the Phe²⁷⁰. Thus, the drug shows 24-fold less activity in a human ovarian carcinoma cell line with the Phe²⁷⁰→Val²⁷⁰ (Phe270Val) mutation. EpoA is located a relatively benign 4 to 5 Å from the same residue and displays only threefold resistance. Taxol experiences substantially less cross-resistance to Thr²⁷⁴ (10-fold) and Arg²⁸² (sevenfold) mutations, in strong contrast to the cellular response to EpoA [40- and 57-fold, respectively] (8, 16)]. In the present model, wild-type Thr²⁷⁴ and Arg²⁸² are cooperatively engaged in a cluster of hydrogen bonds with the C3, C5, and C7 triad of oxygen atoms in EpoA (Fig. 3). Perturbation of either set of noncovalent interactions by elimination of an OH (Thr274Ile) or elonga-

tion of the distance between associated centers (Arg282Gln) dissipates the binding energy between the drug and the protein. The backbone NH of Thr²⁷⁴ is likewise in the vicinity of the oxetane ring of Taxol, such that residue replacement might be expected to diminish ligand binding. However, as has been argued previously (19), this interaction is likely to be weak and not as influential in Taxol's binding. In the epothilone complex, Arg²⁸² is within conformational reach of C7-OH (Figs. 1 and 3). This differs from the tubulin-Taxol complex (13, 20), in which a variation in M-loop conformation directs Arg²⁸² into solvent, but is compatible with the mutation-induced resistance. An acquired mutation reported independently by two groups in lung and leukemia cancer cell lines is the Gln292Glu mutation (70- to 90-fold for EpoA and EpoB) (16, 17). The residue lies on the opposite side of the M-loop from EpoA and makes a hydrogen bond to the backbone NH of Leu²⁷⁵ adjacent to Thr²⁷⁴ (Fig. 3). Interchange of Gln for Glu most likely alters the M-loop conformation, disrupts the network of M-loop hydrogen bonds from Arg²⁷⁸ to Arg²⁸², and thereby prevents epothilone binding. Finally, the present model also explains the Epo-resistant Ala231Thr mutation. Ala²³¹ is within hydrogen bonding contact of His²²⁷, which anchors epothilone in the binding pocket. As has been implied previously (16,

17), the introduction of the polar threonine is predicted to perturb the His anchor and compromise ligand binding.

Our binding model for EpoA accommodates a range of epothilone structure-activity data (6, 21). We show this with the use of six diverse bioactive modifications.

First, alkyl chain extension at C12 from methyl (EpoB) to hexyl does not eliminate *in vitro* activity, although in general methyl appears optimal for biological activity (22, 23). The observation also applies to the desoxy epothilone series in which large groups such as CH₂OC(O)Ph continue to show considerable tubulin polymerizing capacity. The folded orientation of the epoxide (Fig. 1B) directs the C12 substituent into the underlying hydrophobic basin, which readily accepts long and bulky hydrophobic groups. The same observation applies to the epothilone cyclopropanes (24) and cyclobutanes (25) that exhibit high activity (fig. S8).

Second, a more subtle effect is shown by the recently reported epimers of 14-methyl-epothilones B and D (15, 22). The R and S configurations, respectively, exhibit antiproliferative activity against several cell lines that are slightly lower than the parent compounds (epothilones B and D). In contrast, the corresponding S and R configurations are completely inactive. In the bound EC conformation, the active pair directs the methyl group outside the ring into a region unoccupied by protein (Fig. 4). For the inactive pair in the same conformer, the S/R methyl points inward and experiences a severe steric clash with the CH₂ at C10. The associated 1.8 to 2.2 Å H-H distances prevent the molecule from adopting the bound form. For similar reasons, (S)-C10-methyl epothilone C is unable to adopt the bound conformer in accord with its lack of cytotoxicity (15). The model depicted in Fig. 4 predicts that the (R)-enantiomer is active.

Third, the OH at C3 [(3S)-configuration] was replaced with a cyano group in EpoB without substantially altering either the microtubule-stabilizing effect or cell cytotoxicity. Although the OH hydrogen bond to Thr²⁷⁴ is lost, the extension of the C3 substituent by an additional 1.2 Å brings it within favorable H-bonding contact with the backbone NH of Arg²⁷⁶ (Figs. 3 and 4). The tradeoff accounts for the near equipotency with EpoB. By contrast, the unnatural cyano epimer [(3R)-configuration] is 86 times less active in the tubulin polymerization assay (26). The inverted cyano group experiences no undue intra- or intermolecular steric repulsion in the EC model, and it likewise makes no productive contacts. C3-OH inversion would seriously perturb the hydrogen-bonding network shown in Fig. 3.

Fourth, the EC model accommodates active unsaturated Epo analogs. Already mentioned are the cis-EpoC and -EpoD com-

Fig. 2. Superposition of EpoA (blue, C; red, O) and T-Taxol (gold, C; red, O) in β -tubulin as determined by electron crystallography. Hydrogen atoms have been eliminated for clarity. Side chains terminating in aromatic rings occupy distinctly different regions of the binding site. The single common center (<1.1 Å) between the molecules is C7-OH (blue arrows). The image in (A) corresponds to a 90° rotation of the image in (B) about an axis approximately parallel to the blue side chain of EpoA. The alignment shown here without tubulin is identical to those structures shown in Figs. 1 and 3 and figs. S1 to S7.

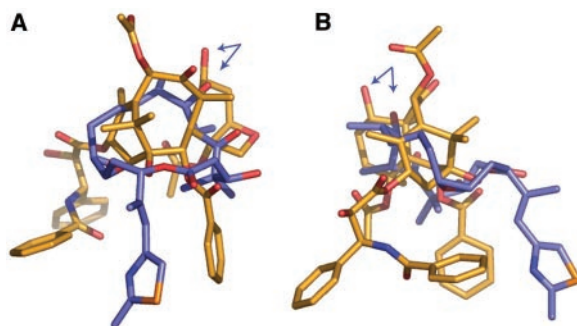
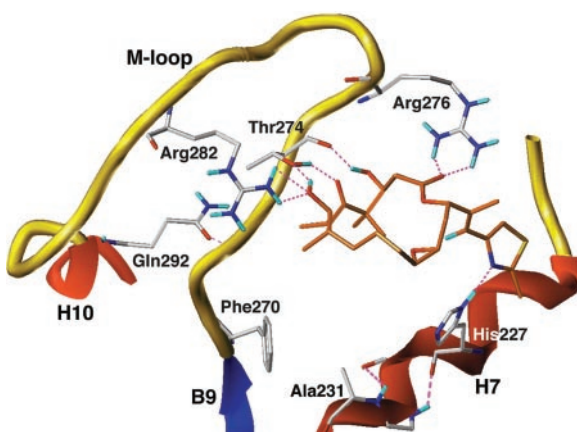


Fig. 3. Hydrogen bonding (violet) around EpoA in β -TB. Oxygens from C1 to C7 engage in network H bonds with M-loop residues. The thiazole is anchored by His²²⁷. Disruption of primary or secondary hydrogen bonds would occur upon mutation of Ala²³¹, Thr²⁷⁴, Arg²⁸², or Gln²⁹² to other residues as observed in epothilone-resistant cells. Protein secondary structure for helices is shown in red, sheets in blue, and loops in yellow. The protein side chains are colored by atom type: white, C; red, O; and blue, N. The EpoA ligand is colored by atom type: orange, C; red, O; blue, N; and yellow, S.



pounds. Conformational analysis for the corresponding trans-analog and docking into the binding site depicted in Fig. 1B assures that this isomer can participate in all key ligand-receptor interactions without steric congestion. Recent synthesis of second-generation epothilones targeted (E)-9,10-dehydro-12,13-desoxy-EpoB, a compound four times as active as desoxy-EpoB against several cell lines (27). The planar and trans C9–C10 center is naturally incorporated by the corresponding trans disposition of the saturated carbons in Figs. 1B and 4. The analog in which the C12 methyl is replaced by the relatively bulky CF_3 is likewise as active as desoxy-EpoB. The folded epoxide directs this group comfortably into the occluded hydrophobic space. Finally, a slight conformational reorganization in the (E)-10,11-dehydro analog is compatible with both our binding model and the twofold reduction in activity relative to EpoA (28).

Fifth, a number of thiazole replacements have been shown to retain or improve epothilone activity. Specifically, Nicolaou and colleagues found that pyridines in which the nitrogen is ortho to the side chain connector are 10

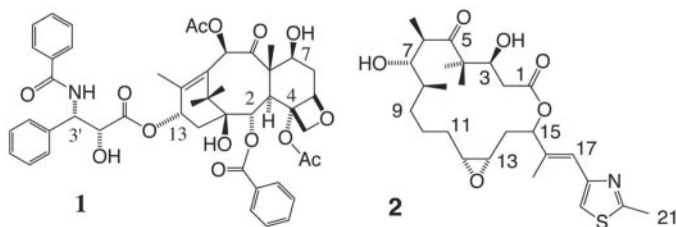
to 100 times more effective in cells than meta and para placement of the heteroatom (25, 29). Figs. 1 and 3 illustrate the origin of the effect to lie in hydrogen bonding of this group to His²²⁷. Other nitrogen placements are unable to anchor the side chain as illustrated. A particularly interesting set of analogs are Altman's benzo-heterocycles, which result from fusion of the methyl at C16 to the terminal heterocycle (Fig. 4) (30). To maintain the H bond to His²²⁷ in this set of analogs, the side chain of bound epothilone must position the C16 methyl and the C19 ring carbon in a syn orientation, and the nitrogen of the EpoB ring anti to the same methyl. The models depicted in Figs. 1 and 3 meet these requirements perfectly. A confirming experiment is the inactivity of a pyridine in which both nitrogen and a methyl substituent are ortho to the side chain connector. Maintenance of the H bond to His²²⁷ would involve a severe steric clash between the pyridine methyl and that at C16. Obviously, the compound cannot adopt the proposed active conformation, consistent with its virtual inactivity against all cell lines (29). A particularly productive variation leading to an EpoB analog more active than the parent is replacement of the thiazole methyl at C21

with thiomethyl (SMe). In the present model, the SMe fits snugly into a small, shallow pocket unsuitable for larger substituents (Fig. 4). Accordingly, increased bulk diminishes activity (30).

Sixth, a series of active epoxide replacements in the form of aziridines has been prepared (31). For example, the bulky NCOOC_6H_5 and NCOC_6H_5 analogs show a tubulin polymerization and antiproliferative activity profile virtually identical to that of EpoB. The terminal phenyl rings are unlikely to be directed toward the surface of the protein exposed to water. Once again, the folded epoxide accommodates the observations by steering the N-substituent beneath the macrocyclic ring into the hydrophobic taxoid pocket (Fig. 4).

The SAR data described for the extended C12 substituents, epothilone cyclopropanes, and the aziridines suggests that the epothilone 16-membered ring and part of the side chain resides over a spacious but unfilled hydrophobic pocket on tubulin. Indeed, the present EpoA/tubulin model includes a generous cavity between the epothilone structure and the floor of the hydrophobic pocket surrounding Phe²⁷⁰. The cavity is likely filled with water molecules that are either displaced or reorganized upon binding by a substituted epothilone but are unobservable at ~ 3 Å resolution.

In the EC model, EpoA that is bound to tubulin is anchored at two extremes by hydrogen bonds. C1=O, C3-OH, C5=O, and C7-OH on one flank of the molecule participate in a network of short contacts with Thr²⁷⁴, Arg²⁷⁸, and Arg²⁸², residues on the M-loop, and nitrogen in the 10.5 Å distal thiazole ring serves as a proton acceptor for His²²⁷ (Fig. 3). The remaining ligand-protein contacts are primarily hydrophobic, providing a tight surface-to-surface interaction from C3 to C11 (Fig. 1B). The Taxol-TB contacts are fundamentally different (fig. S6). The two phenyl C13 side chain termini and the C2' OH group associate with TB centers distant from epothilone (i.e., Ser²³⁴/Pro³⁵⁸, Val²¹, and Gly³⁶⁸, respectively), whereas the C2 and C3' phenyl groups sandwich His²²⁷ in a three-ring stack (13), neither set of contacts is observed for epothilone. The ether oxygen of Taxol's oxetane ring interacts weakly with Thr²⁷⁴ at one end of the M-loop, whereas an indirect hydrophobic chain to the other end operates by means of the C18 methyl. As mentioned above, the only notable common nonbonded contact for the two ligands appears to occur through C7-OH in each molecule. For T-Taxol, this affords a long and weak polar interaction with the C-OH of Thr²⁷⁴; for EpoA, it allows classic H bonds to Thr²⁷⁴ and Arg²⁸⁴. Although M-loop arginines 278 and 282 in Taxol-TB are directed toward solvent (13), both have shifted by 6 to 8 Å in



Scheme 1.

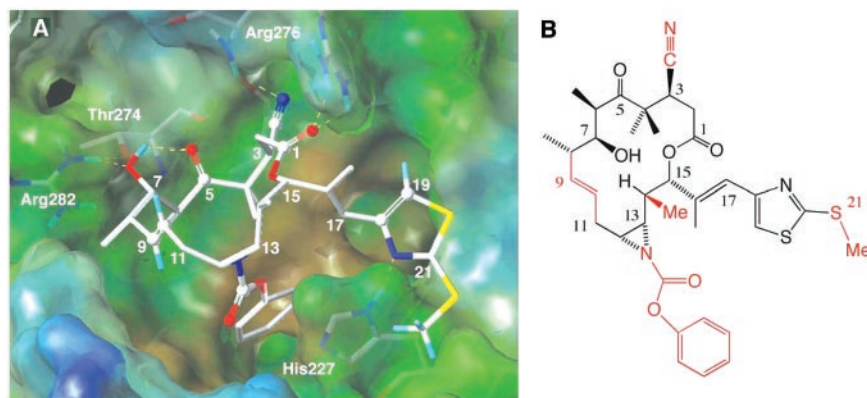


Fig. 4. An energy-optimized composite model of a fictionalized epothilone showing diverse features of the SARs in the context of the EC-derived model for TB and epothilone A. This single ligand structure docked into β -tubulin incorporates functional group modifications from five different analog studies that individually produced the same or better potency than epothilone A, including effects caused by changes of functionality at C3 (CN), C9–C10 (C=C), C12–C13 (N-Bz-aziridine), C14 ((S)-Me), and 21 (SMe). **(A)** The experimental conformation and binding mode of **1** in Figs. 1 to 3 used as a modeling template to illustrate geometric compatibility (C9=C10, C14-Me), hydrogen bonds (C3-CN), and hydrophobic complementarity (aziridine phenyl, S21-Me) for the five derivatives. Colors on the translucent protein surface range from brown (hydrophobic) to blue (hydrophilic). The ligand is colored by atom type: white, C; red, O; blue, N; and yellow, S. **(B)** Topological representation of the composite model; red corresponds to the five centers of substitution relative to epothilone A.

the Epo-TB complex so as to engage epothilone (Fig. 3). A similar arginine displacement (4 Å) has been observed in the binding of two epothilones to cytochrome P450-EpoK (32). The double arginine relocation reflects a subtle reorganization of M-loop residues not previously seen with taxanes, but both epothilone and Taxol bridge the M-loop and helix H7 adjacent to the nucleotide-binding site and thereby promote tubulin polymerization and microtubule stability.

Instead of a common pharmacophore (8–11), tubulin displays a promiscuous binding pocket with the bound molecules exploiting contacts with an optimal subset of binding pocket residues. Although this provides a unique challenge for “rational” ligand design, it can be anticipated that the promiscuity principle will apply to the binding of other ligands that occupy the taxane site on TB, namely, discodermolide, eleutherobin, and the sarcodictyins (33).

References and Notes

1. A. K. Singla, A. Garg, D. Aggarwal, *Int. J. Pharm.* **235**, 179 (2002).
2. M. M. Gottesman, *Annu. Rev. Med.* **53**, 615 (2002).
3. J. P. Guastalla, V. Diéras, *Br. J. Cancer* **89**, S16 (2003).
4. G. Höfle, N. Bedorf, K. Gerth, H. Reichenbach, *Chem. Abstr.* **120**, 52841 (1993).
5. D. Bollag et al., *Cancer Res.* **55**, 2325 (1995).
6. M. Wartmann, K. H. Altmann, *Curr. Med. Chem. Anti-Cancer Agents* **2**, 123 (2002).
7. S. Kar, J. Fan, M. J. Smith, M. Goedert, L. A. Amos, *EMBO J.* **22**, 70 (2003).
8. L. He et al., *Biochemistry* **39**, 3972 (2000).
9. P. Giannakakou et al., *Proc. Natl. Acad. Sci. U.S.A.* **97**, 2904 (2000).
10. M. Wang et al., *Org. Lett.* **1**, 43 (1999).
11. I. Ojima et al., *Proc. Natl. Acad. Sci. U.S.A.* **96**, 4256 (1999).
12. Materials and methods are available as supporting material on Science Online.
13. J. P. Snyder, J. H. Nettles, B. Cornett, K. H. Downing, E. Nogales, *Proc. Natl. Acad. Sci. U.S.A.* **98**, 5312 (2001).
14. T. Carlomagno et al., *Angew. Chem. Int. Ed. Engl.* **42**, 2511 (2003).
15. R. E. Taylor, Y. Chen, G. M. Galvin, P. K. Pabba, *Org. Biomol. Chem.* **2**, 127 (2004).
16. L. He, C.-P. H. Yang, S. B. Horwitz, *Mol. Cancer Ther.* **1**, 3 (2001).
17. N. M. Verrills et al., *Chem. Biol.* **10**, 597 (2003).
18. P. Giannakakou et al., *J. Biol. Chem.* **272**, 17118 (1997).
19. M. Wang, B. Cornett, J. Nettles, D. C. Liotta, J. P. Snyder, *J. Org. Chem.* **65**, 1059 (2000).
20. J. Lowe, H. Li, K. H. Downing, E. Nogales, *J. Mol. Biol.* **313**, 1045 (2001).
21. K. C. Nicolaou, F. Roschangar, D. Vourloumis, *Angew. Chem. Int. Ed. Engl.* **37**, 2014 (1998).
22. R. E. Taylor, Y. Chen, A. Beatty, D. C. Myles, Y. Zhou, *J. Am. Chem. Soc.* **125**, 26 (2003).
23. K. C. Nicolaou, A. Ritzén, K. Namoto, *Chem. Commun.* **2001**, 1523 (2001).
24. J. Johnson et al., *Org. Lett.* **2**, 1537 (2000).
25. K. C. Nicolaou et al., *J. Am. Chem. Soc.* **123**, 9313 (2001).
26. A. Regueiro-Ren et al., *Org. Lett.* **4**, 3815 (2002).
27. A. Rivkin et al., *J. Am. Chem. Soc.* **125**, 2899 (2003).
28. I. H. Hardt et al., *J. Nat. Prod.* **64**, 847 (2001).
29. K. C. Nicolaou et al., *Chem. Biol.* **7**, 593 (2000).
30. K. C. Nicolaou et al., *Angew. Chem. Int. Ed. Engl.* **42**, 3515 (2003).
31. A. Regueiro-Ren et al., *Org. Lett.* **3**, 2693 (2001).
32. S. Nagano et al., *J. Biol. Chem.* **278**, 44886 (2003).
33. J. Jimenez-Barbero, F. Amat-Guerri, J. P. Snyder, *Curr. Med. Chem. Anti-Cancer Agents* **2**, 91 (2002).
34. Supported in part by NIH and the Department of Energy. J.N., B.C., and J.P.S. thank D. Liotta (Emory University) for encouragement, discussion, and support during the course of the work. We thank P. Giannakakou, J. Gallivan, and D. Lynn (Emory University) for helpful discussions. Structure has been deposited in the Protein Data Bank under accession number 1TVK.

Supporting Online Material

www.sciencemag.org/cgi/content/full/305/5685/866/DC1
Materials and Methods
Figs. S1 to S8
References

15 April 2004; accepted 12 July 2004

Multiple Rare Alleles Contribute to Low Plasma Levels of HDL Cholesterol

Jonathan C. Cohen,^{1,2,3,*†} Robert S. Kiss,^{5*}
Alexander Pertsemlidis,¹ Yves L. Marcel,^{5†} Ruth McPherson,⁵
Helen H. Hobbs^{1,3,4}

Heritable variation in complex traits is generally considered to be conferred by common DNA sequence polymorphisms. We tested whether rare DNA sequence variants collectively contribute to variation in plasma levels of high-density lipoprotein cholesterol (HDL-C). We sequenced three candidate genes (*ABCA1*, *APOA1*, and *LCAT*) that cause Mendelian forms of low HDL-C levels in individuals from a population-based study. Nonsynonymous sequence variants were significantly more common (16% versus 2%) in individuals with low HDL-C (<fifth percentile) than in those with high HDL-C (>95th percentile). Similar findings were obtained in an independent population, and biochemical studies indicated that most sequence variants in the low HDL-C group were functionally important. Thus, rare alleles with major phenotypic effects contribute significantly to low plasma HDL-C levels in the general population.

Many clinically important quantitative traits are highly heritable, but progress in the elucidation of their genetic architecture has been limited. Because quantitative traits do not segregate in Mendelian fashion in most families, their distribution in the population is presumed to reflect the cumulative contribution of multiple common DNA sequence variants that each has a small effect (1). Sequence variants with strong phenotypic effects may also contribute to variation in complex traits (2). Although these variants

are likely to be rare individually, they may be sufficiently common in aggregate to contribute to variation in common traits in the population. Whereas most Mendelian disorders are caused by a spectrum of different mutations in a gene (or genes) (3), the contribution of rare alleles to more common, quantitative traits has not been systematically evaluated.

In this study, we evaluated the hypothesis that rare sequence variations contribute significantly to low plasma levels of high-density lipoprotein cholesterol (HDL-C), a

major risk factor for coronary atherosclerosis. If this hypothesis is correct, then mutations that impair HDL production or enhance HDL catabolism should be significantly more common among individuals with low plasma levels of HDL-C than among those with high plasma levels of HDL-C. Furthermore, sequence variants with major phenotypic effects are likely to be found exclusively at one extreme or the other, whereas alleles found in both the high HDL-C and the low HDL-C groups are likely to be neutral with respect to plasma HDL-C levels. The prevalence of mutations with major effects on plasma HDL-C levels is not known. Molecular defects causing rare genetic forms of HDL deficiency have been identified in the genes encoding apolipoprotein AI (*APOA1*), the major protein component of HDL (4); the adenosine triphosphate binding cassette (ABC) transporter A1 (*ABCA1*), required for the efflux of cholesterol from cells to HDL particles (5); and lecithin cholesterol acyltransferase (*LCAT*), the enzyme that catalyzes the formation of

¹Donald W. Reynolds Cardiovascular Clinical Research Center and McDermott Center for Human Growth and Development, ²Center for Human Nutrition, ³Department of Internal Medicine and Department of Molecular Genetics, ⁴Howard Hughes Medical Institute, University of Texas Southwestern Medical Center, Dallas, TX, 75390, USA. ⁵Lipoprotein and Atherosclerosis Research Group, University of Ottawa Heart Institute, Ottawa, Ontario K7Y4W7, Canada.

*These authors contributed equally to this work.

†To whom correspondence should be addressed. E-mail: jonathan.cohen@utsouthwestern.edu (J.C.C.); ymarcel@ottawaheart.ca (Y.L.M.)